ISSN 2228-9860 eISSN 1906-9642 CODEN: ITJEA8

International Transaction Journal of Engineering, Management, & Applied Sciences & Technologies

http://TuEngr.com

Biodecolorization of Reactive Dyes Using Biochar Derived from Rice Husk (*Oryza Sativa*): Batch & Isotherm and Kinetic & Desorption Studies

R. Muralikrishnan[1*], C. Jodhi[1]

[1] Department of Civil Engineering, Annamalai University, Tamil Nadu, 608002, INDIA.
**Corresponding Author (Tel: +91-9655223113, Email: murali660105@gmail.com).*

Paper ID: 12A8D

Volume 12 Issue 8

Received 08 March 2021
Received in revised form 15 May 2021
Accepted 25 May 2021
Available online 02 June 2021

Keywords:
Rice husk-derived biochar; Reactive dyes; Elutants; Freundlich model; Dye removal by adsorption; S/L ratio; Synthesis of Biochar; FTIR Spectrum; Freundlich adsorption isotherm; Pseudo-first-order kinetic model; Pseudo-second-order kinetic model; Desorption efficiency; Dye uptake capacity; Adsorption isotherm.

Abstract

This study assesses how rice husk biochar is used to remedy three reactive dyes including Reactive Black 5 (RB5), Reactive Orange 16 (RO16), and Reactive Blue 19 (RB19) in an aqueous solution. From the batch study, it is understood that the dye gets adsorbed at the maximum level when the pH is 2, the temperature is 35°C and the biochar dosage is maintained at 1 g/l. The adsorption isotherm experiments determined the highest uptakes of RO16, RB5, and RB19 to be 73.44 mg/g, 75.68 mg/g, and 55.37 mg/g, respectively. Freundlich Model is considered as the best fit model based on Isotherm studies that had a correlation coefficient of more than 0.9570. The kinetic study signifies that maximum adsorption has been completed within 120 minutes whereas two models such as pseudo-first-order kinetic model and pseudo-second-order kinetic model were utilized to fit the experimental data. This study reports the investigation on biochar reusability with the help of different elutants, S/L ratios, and regeneration cycles.

Disciplinary: Environmental Engineering & Management, Environmental Chemical Engineering, Pollution & Detoxification, Bioresources.

Cite This Article:

Muralikrishnan, R., Jodhi, C. (2021). Biodecolorization of Reactive Dyes Using Biochar Derived from Rice Husk (Oryza Sativa): Batch & Isotherm and Kinetic & Desorption Studies. *International Transaction Journal of Engineering, Management, & Applied Sciences & Technologies, 12*(8), 12A8D, 1-15. http://TUENGR.COM/V12/12A8D.pdf DOI: 10.14456/ITJEMAST.2021.151

1 Introduction

Dyes are mostly consumed in industries that manufacture paint, textiles, paper, pulp, and tanneries. Thus, the prominent effluent expelled from these industries remains dye [1]. The organic pollutants released from these industries affect the water quality and cause irreversible damage. In recent times, removal of dyes is made possible through different physical as well as chemical

treatment methods namely, reverse osmosis, coagulation-flocculation, chemical precipitation, ion exchange, biodegradation, etc. But these treatment methods are less result-oriented in the complete removal of dye, since the latter possesses vibrant physical and chemical properties [2]. Further, dyes used in textile industries do not get completely adhered to fabrics. In other terms, it gets washed away and pollutes the water bodies directly [3]. Dyes, being inorganic in nature possess carcinogenic properties and thus harm the environment if discharged directly without treatment. Comparatively, the composition of textile industry wastewater is diverse and complex, thanks to different varieties of dyes [4]. Complex wastewater does not get completely remediated since modern technologies do not focus on individual dyes. So, adsorption has become the most notable and prevalently used dye remediation method. Adsorption treatment is a superior method thanks to its efficiency, economical approach, and simple production procedure [5]. The solution (wastewater containing dye) is exposed to a sorbent in a batch or continuous process, resulting in high-quality water. Both inorganic and organic sorbents of various types are used for the treatment process. Among the adsorbents available, activated carbon is the most prevalently used adsorbent, owing to its huge surface area and thermostability [6, 7]. However, the activated carbon process incurs heavy costs and remains unaffordable for wastewater treatment. In this scenario, low-cost naturally-available adsorbents started gaining attention among researchers in biochar synthesis (8, 9). Being a carbon-rich material, biochar is manufactured without the presence of oxygen under the thermal decomposition process. The process is inclusive of slow pyrolysis and fast pyrolysis or hydrothermal carbonization [10]. Biochar possesses a huge surface area with different pore sizes and numerous functional groups, for instance, carboxyl, carbonyl, and phenolic compounds [11]. Biochar is an established adsorbent nowadays, thanks to its vibrant features, easy-to-use nature, in remedying numerous dyes and heavy metals [10, 11, 12, 13]. Jegal et al conducted a study in which cationic dyes such as basic blue 41 and basic red 41 were successfully remedied by groundnut shell-based biochar and its uptake values were 22.32 mg/g and 40.65 mg/g respectively [15]. This study assessed how far it is feasible to remedy the reactive dyes such as Reactive Black 5 (RB5), Reactive Orange 16 (RO16), and Reactive Blue 19 (RB19) with the help of rice husk-based biochar in an aqueous solution. Biochar from rice husk is synthesized by slow thermal pyrolysis.

2 Materials and Methods

2.1 Synthesis of Biochar

The agricultural waste rice husk was collected from the paddy fields (Chidambaram, Tamilnadu). The collected rice husk was manually cleaned and soaked in distilled water for 30 minutes to remove the impurities. The rice husk was naturally dried by exposing it to the atmosphere for 24 hours. It was further dried in a hot air oven for up to 24 hours at 103°C. Later, the rice husk was shredded to obtain a particle size of 0.75cm for further processing. A measured amount (100g) of dried sample was taken in a crucible, which is closed with an aluminium foil possessing two small holes. Then, it was kept in a muffle furnace for two hours at 450°C at a 5°C

/minute heating rate. In the beginning, the muffle furnace was purged with Nitrogen gas at 100 ml/min for 15 minutes to ensure the absence of oxygen in the furnace. After the furnace reached room temperature, the sample was taken out and was maintained in a desiccator for further studies.

2.2 Dyes and Chemical

This study used three reactive dyes including Reactive Black 5 (RB5), Reactive Orange 16 (RO16), and Reactive Blue 19 (RB19). Table 1 shows the characteristics of dyes used in the study. This study used analytical-grade chemical agents bought from Sigma-Aldrich (India).

Table 1: Characteristics of different Reactive Dyes.

Dyes	Empirical formula	Colour index	Molecular weight (g/mg)	λmax (nm)
Reactive orange 16 (RO16)	C20H17N3Na2O11S3	17757	617.54	490
Reactive Black 5 (RB5)	C26H21N5Na4O19S6	20505	991.82	597
Remazol brilliant blue R (RB19)	C22H16N2Na2O11S3	61200	626.54	595

2.3 Analytical Methods

The thermogravimetric analyser (TG-DSC / NETZSCH STA 449 F3 Jupiter) is used to understand the thermal decomposition of the sample during the pyrolysis process. The analysis was performed by using 8.318 mg of raw rice husk as sample mass and 7.668 mg of alumina as a reference under an inert environment using nitrogen as a protective gas at 20 ml/minute flow rate from 0-700°C whereas its heating rate was maintained at 5 °C/min. Surface morphology of biochar before and after treatment is observed for all samples using Scanning Electron Microscopy (SEM) incorporated with Energy Dispersive Spectroscopy (EDS) (FEI-Quanta FEG 200F). At first, coating the samples with gold (thin layer) was executed. Fourier Transform Infrared (FT-IR) spectrophotometer (Bruker-FTIR / ATR) was used to confirm the surface functional group changes prior to and after the treatment. Between 500-400 cm^{-1}, the spectra were recorded and the samples were mixed with KBr to form pellets prior to analysis.

2.4 Isotherm and Kinetic Models

Three different forms of isotherm models were utilized, including

Freundlich model: $$Q = K_F C_e^{1/n_F} \quad (1),$$

Langmuir model: $$Q = \frac{Q_{max} b_L C_e}{1 + b_L C_e} \quad (2),$$

Toth model: $$Q = \frac{Q_{max} b_T C_e}{[1 + (b_T C_e)^{1/n_T}]^{n_T}} \quad (3).$$

The symbol n_F denotes Freundlich model exponent and K_F denotes Freundlich model (mg/g) coefficient. (L/mg)$1/n_F$, Qmax corresponds to the sorbent's maximum dye uptake (mg/g), b_L denotes the Langmuir model (L/mg) equilibrium coefficient, b_T denotes Toth model (L/mg) constant and nT corresponds to Toth model exponent.

Equations (4) and (5) denote pseudo-first- and -second-order kinetic models used for kinetic studies.

Pseudo-first order model: $$Q_t = Q_e(1-\exp(-k_1 t)) \quad (4)$$

Pseudo-second order model: $$Q_t = \frac{Q_e^2 k_2 t}{1+Q_e k_2 t} \quad (5)$$

Q_e denotes the equilibrium dye uptake capacity (mg/g), Qt denotes the dye uptake capacity at any time t (/g), k_1 (1/min) and k_2 (g/mg.min) are the rate constants of pseudo-first and pseudo-second-order models, respectively.

2.5 Batch Studies

For the batch adsorption study, a 250ml Erlenmeyer flask with 100ml working volume was used. The flask was continuously mixed in a temperature-controlled rotating orbital shaker at 200 rpm for an equilibrium time of 360 minutes. Once the equilibrium adsorption study is completed, the suspension in the flask was kept under centrifugation at 2500 rpm for 10 minutes. The concentration of dye was quantified with the help of a spectrophotometer at respective dye wavelengths (λ max) as given in Table 1. Similarly, parameters were varied and the adsorption studies were carried out.

2.6 Regeneration Studies

Several eluting agents were investigated to check whether biochar can be reused for another adsorption cycle. In this attempt elutants, like 0.1 M of sodium hydroxide (NaOH), sodium carbonate (Na_2CO_3), ammonium hydroxide (NH_4OH), hydrochloric acid (HCl), and Methanol (CH_3OH) were utilized to assess the biochar's desorption efficiency. The researcher conducted desorption studies alike adsorption studies. Further, different elutant volumes were used to study the impact of the solid/liquid (S/L) ratio. These will give the optimum amount of elutant to be used for the desorption studies. The sorption-elution process was also studied to check the capacity of the biochar in the continuous sorption-elution process.

3 Result and Discussion

3.1 Thermogravimetric Analysis

The researcher conducted thermogravimetric analyses to investigate the influence of pyrolysis on raw rice husk biomass samples. Figure 1 shows the degradation curve which infers that the sample weight got reduced with increasing temperature (Figure 1). At 699°C, a total weight loss of 67.83% was observed. Rice husk underwent thermal decomposition in three stages among which the first stage observed a mass change of 9.90% between 0-100°C which might be attributed to moisture loss. Between 100-350°C i.e., second stage, a mass change of 34.21% was observed. This is the most crucial degradation zone during pyrolysis since maximum decomposition of cellulose, hemicellulose, and lignin occurs in this stage [19]. The final stage that occurs between 350°C-500°C

was the last decomposition zone during when cellulose, hemicellulose, and lignin got completely decomposed which can be understood from the mass change of 24.77%. Further, the flat curve was obtained at 699°C with 32.17% leftover mass. As per the analysis, between 0-699°C, the overall mass change observed was 67.83%. In the case of the DSC curve, the peak value was attained at 438.8°C temperature which is in line with the Pyrolysis temperature chosen for biochar synthesis.

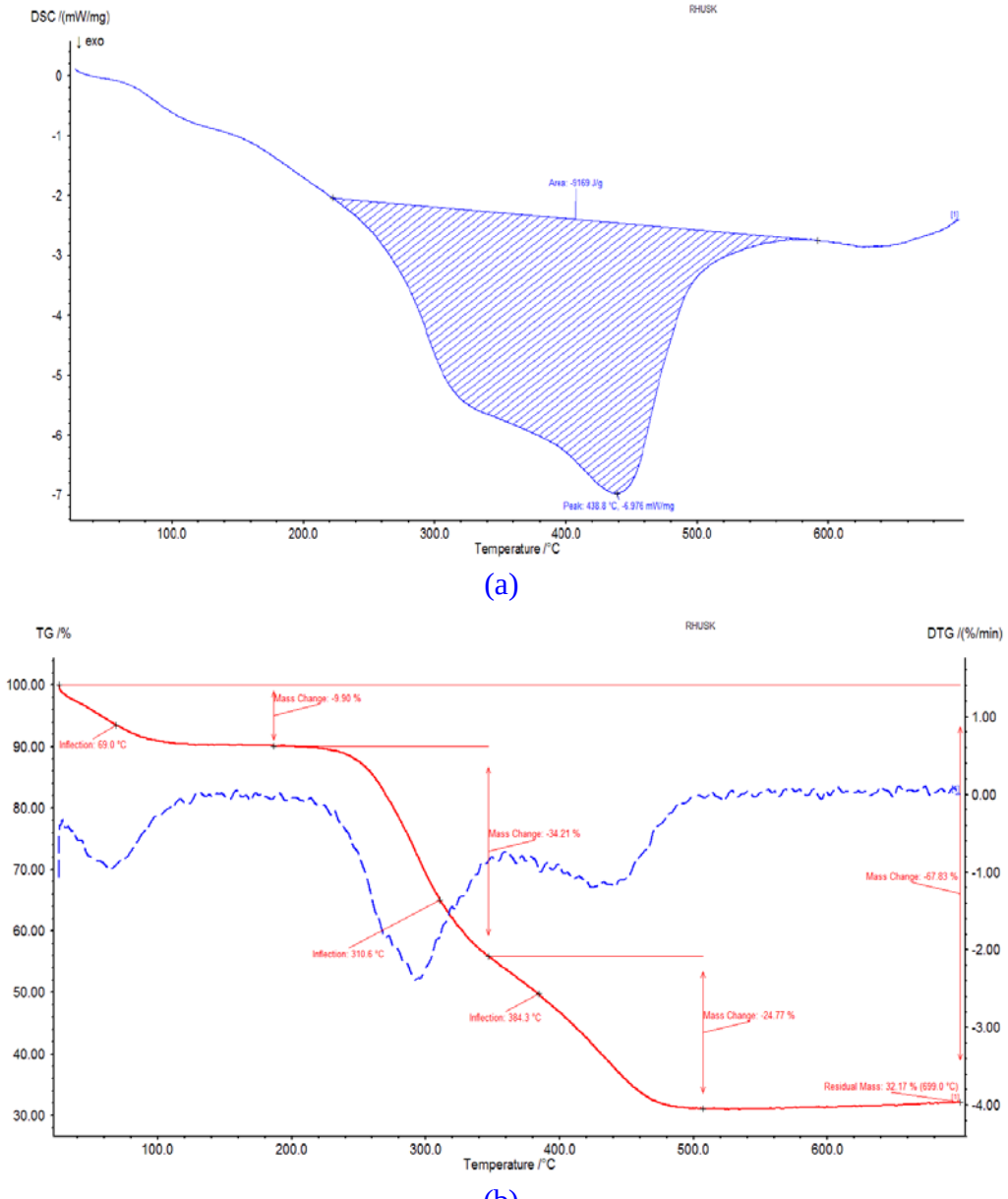

Figure 1: Thermal Analysis of Raw husk - DIGITAL Scanning Colorimetry (a); Digital Thermogravimetric (b).

3.2 Scanning Electron Microscopy with Energy Dispersive Spectroscopy

Figure 2 shows scanning electron microscope images that display the surface morphological characteristics of reactive dyes-bounded biochar. The figure infers the presence of a rough surface upon rice husk-based biochar with numerous pores. These pores act as the active binding site and maximize the surface area to achieve the highest uptake of reactive dyes during adsorption. It is to be noted that the biochar surface got considerably changed after reactive dye adsorption which might be attributed to the ion exchange that occurred between biochar and reactive dyes.

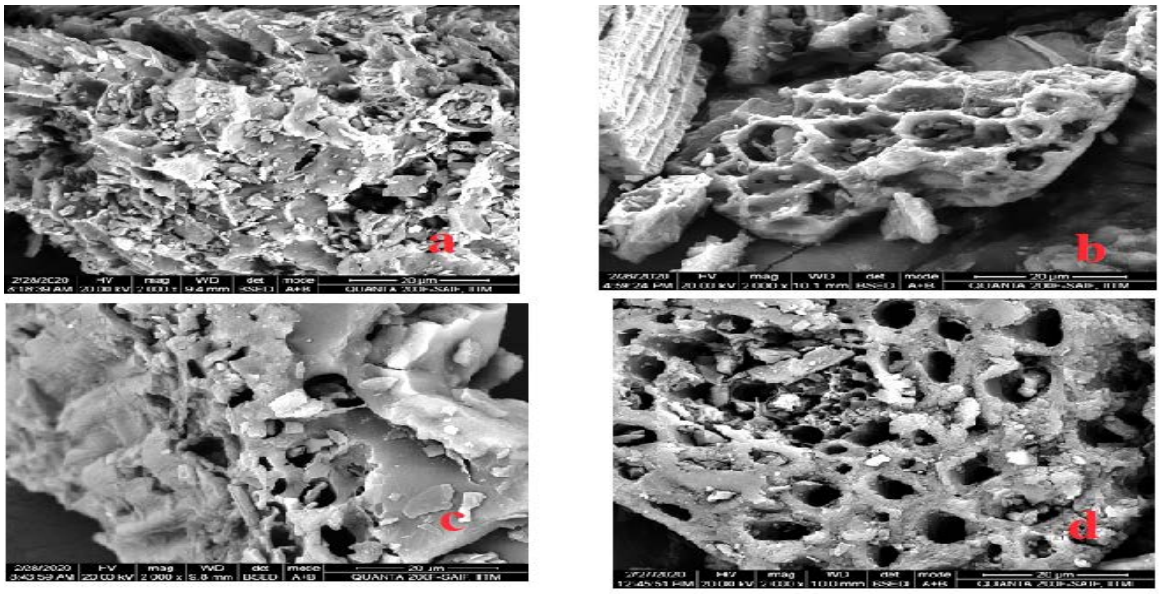

Figure 2: SEM images of rice husk-derived biochar (a); RO16 bounded biochar (b); RB5 bounded biochar(c); RB19 bounded biochar (d).

In Figure 3, the researcher shows the raw biochar's Energy Dispersive Spectroscopy (EDS) spectra and reactive dye-bounded biochar. It is inferred from the figure that the raw biochar composition is mostly carbon (77.42%) and oxygen (17.64%). This is attributed to the decarboxylation and dehydration of aliphatic and hydroxy groups at maximum pyrolysis temperature (18). For biochar to have a maximum adsorption capacity, the carbon content of the adsorbent has to be at its maximum. After the adsorption process is over, a significant quantity of carbon got decreased. The carbon content of 77.08%, 76.09%, and 60.71% is observed for RB19, RB5, and RO16.

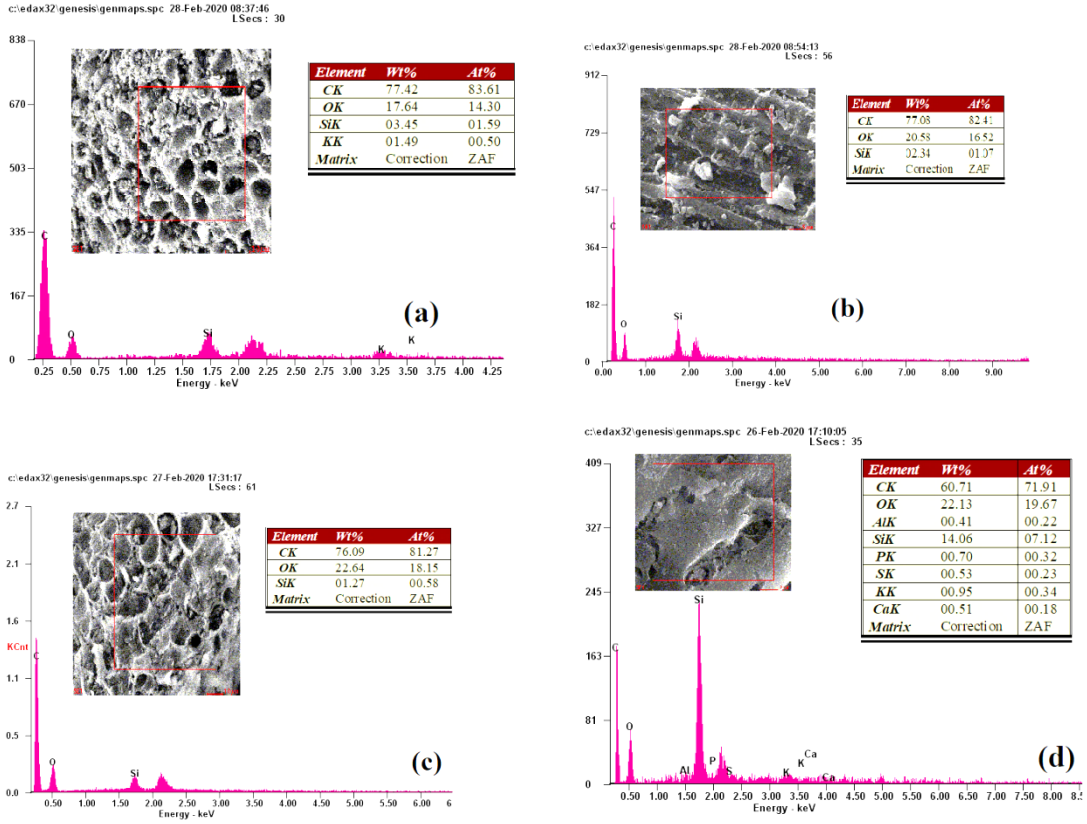

Figure 3: EDS of Raw Rice Husk-derived biochar (a); RB19 bounded biochar (b); RB5 bounded biochar(c); RO16 bounded biochar (d).

3.3 FTIR Spectrum

Figure 4 shows the FTIR spectra of both raw and reactive dye-bound biochar. The figure infers that numerous peaks are present in biochar which exhibits its complexity. Strong bands were exhibited in the FTIR spectra of raw rice husk-derived biochar at 654.16 (=C-H bend), 1071.09 (C-O stretch), 1697.17 (C=C Stretch), 2110.44 (N-H bend), 2921.04 (O-H stretch), 3309.26 (C-H bend). A functional difference was understood between raw- and reactive dyes-bound biochar from FTIR spectra after the adsorption process is over. For example, a peak was observed in FTIR spectra of RB5-bounded biochar at 791.49 (=C-H bend), 1368.68 (C-O stretch), 1704.71 C=C Stretch), 2107.46 (N-H bend), 2852.62 (O-H stretch), 3316.06 (C-H bend), respectively. At the time of reactive dye adsorption, key shifts have occurred and are presented in Table 2.

Table 2: FT IT Spectra of raw biochar and reactive dyes bounded biochar.

Type of Vibration	Characteristic Adsorption (cm^{-1})			
	Raw Rice Husk derived biochar	RB5 bounded biochar	RB19 bounded biochar	RO16 bounded biochar
=C-H bend	654.16	791.49	608.63	791.41
C-O stretch	1071.09	1368.68	1042.74	1049.41
C=C stretch	1697.17	1704.71	1701.95	1700.88
N-H bend	2110.44	2107.46	2110.47	2106.65
O-H stretch	2921.04	2852.62	2921.24	2924.37
C-H bend	3309.26	3316.06	3248.10	3252.68

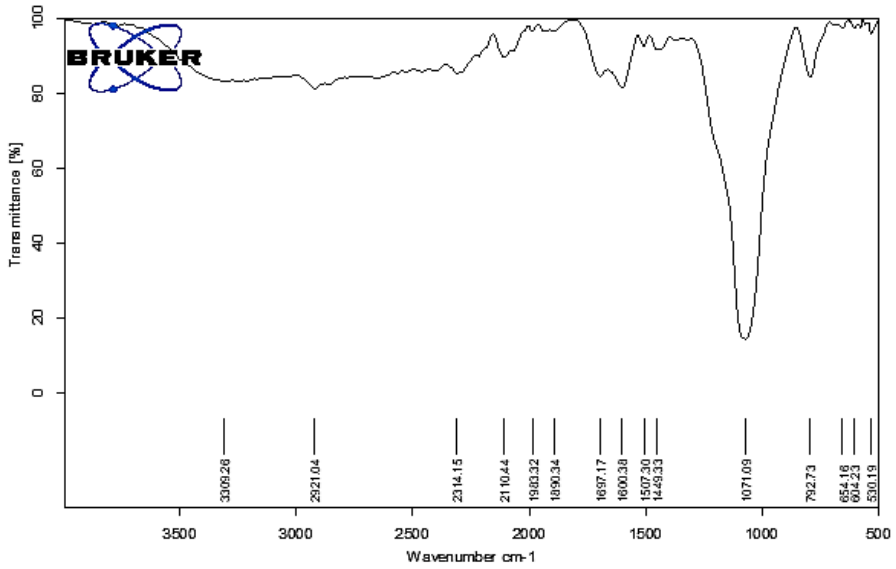

Figure 4: The FTIR spectra of raw rice husk.

3.4 Effect of Biochar Dosage

Figure 5 shows the impact of dosage of rice husk-derived biochar upon RO16, RB5, and RB19 dyes adsorption. The researcher tested different dosages from 0.5 g/L to 10 g/L to find the optimum dosage for maximum removal and uptake capacity of biochar. At the time of conducting the batch study, pH was maintained at 2, the temperature at 35°C, and the initial concentration at 15 mg/L. Figure 5 concludes that the dye adsorption capacity of biochar gets increased with increasing biochar dosage, while the dye uptake capacity gets decreased with increasing biochar dosage. For example, there was an increase in the removal efficiency of RO16, RB5, and RB19 from 62.53-84%,

39.27-69.27%, and 42.47-72.47% when biochar dosage was increased from 0.5 g/L to 10 g/L. Further, figure 5 infers that there was a decline in the uptake capacity of RO16, RB5, and RB19 from 18.76 mg/g to 1.26 mg/g, 11.78 mg/g to 1.04 mg/g, and 12.74 mg/g to 1.09 mg/g respectively. This might be due to less number of binding sites with low biochar dosage in the presence of excess dye concentration [16]. This scenario ensures the maximum uptake capacity of dye per unit mass of biochar [17]. Contrarily, when biochar dosage is high, the overall uptake capacity remains low, owing to the presence of excess binding sites against low dye concentration [18]. It is to be noted that removal efficiency and biochar mass utilized are independent of each other. The biochar dosage of 1 g/L is considered as the optimum value for further batch trials based on biochar uptake capacity and dye removal efficiency.

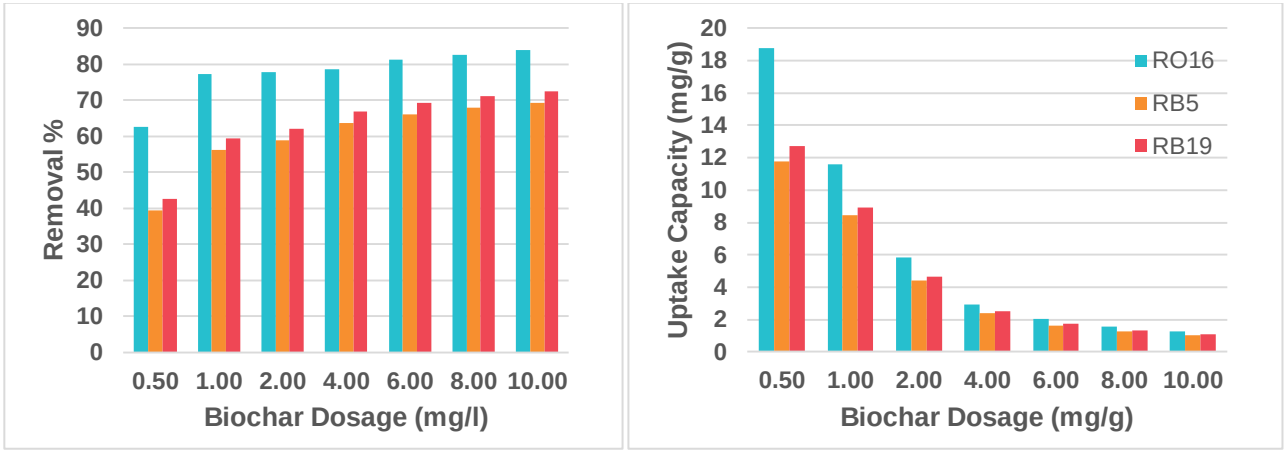

(a) (b)

Figure 5: Effect of Biochar dosage on the removal efficiency (a) and Uptake capacity of different reactive dyes (b).

3.5 Effect of pH

The pH of the dye solution changes the biochar's surface chemistry due to which the latter's uptake capacity varies [19]. So, the impact of dye solution pH upon dye removal efficiency was analyzed by introducing different equilibrium pH values in the range of 2-5. The parameters such as biochar dosage, temperature, and initial dye concentration were maintained at 1 g/L, 35°C, and 15 mg/L. Figure 6 infers a decline in removal efficiency and uptake capacity of biochar when the solution's pH got increased. For instance, when pH was varied between 2-5, there was a decline in uptake capacity of biochar for RO16, RB5, and RB19 such as 11.58 mg/g to 8.60 mg/g, 8.42 mg/g to 6.52 mg/g/ and 8.90 mg/g to 7.00 mg/g. Further, a decline in dye removal efficiency was also observed from 77.20% to 57.33%, 56.13% to 43.47%, and 59.33% to 46.67% respectively. The surface of biochar gets protonated with more H+ ions which may be the reason behind high removal efficiency and uptake capacity at heavy acidic pH since it provides a positive charge to the biochar surface [19]. Likewise, reactive dyes exist in the solution as anions [20]. Since, naturally, oppositely charged ions attract one another, the highest uptake occurred at least pH as shown in Figure 6. Figure 6 concludes 2 as the optimum pH for good dye removal efficiency and maximum uptake of biochar.

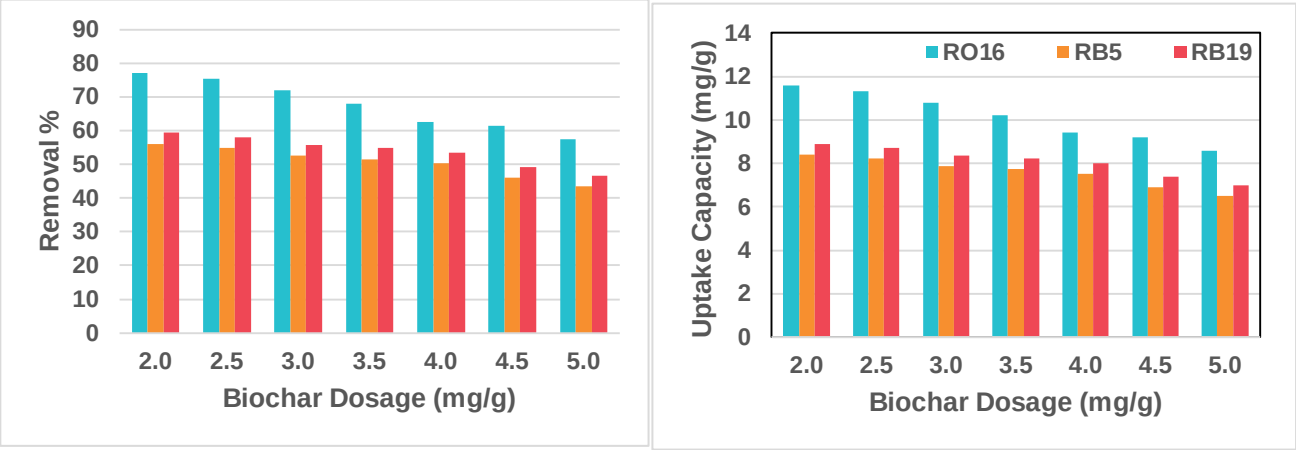

(a) (b)

Figure 6: Effect of pH on the removal efficiency (a) and uptake capacity of different reactive dyes (b).

3.6 Effect of Temperature

Under constant conditions such as pH 2, biochar dosage 1 g/L, and initial dye concentration being 15 mg/L, the researcher analyzed the impact of different temperatures between 35°C to 45°C upon adsorption of reactive dyes on to rice husk-based biochar. Figure 7 infers that when the temperature was increased, the uptake capacity and dye removal efficiency got declined. This might be attributed to increased diffusion rate at high temperatures that impact the adsorption process and vice versa [21]. With varying temperatures in the range of 35-45°C, the uptake capacities of biochar for RO16, RB5, and RB19 were as follows, 11.58 mg/g to 10.42 mg/g, 8.42 mg/g to 3.41 mg/ and 8.24 mg/g to 3.89 mg/g. So, the researcher concludes that 35°C is the optimum temperature for maximum dye removal.

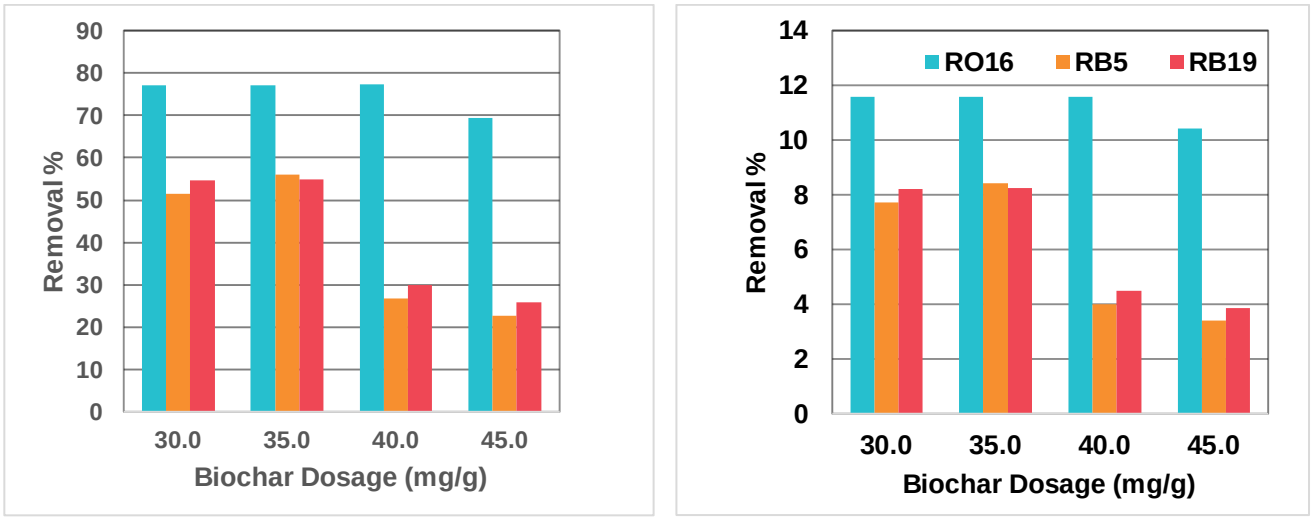

(a) (b)

Figure 7: Effect of temperature on the removal efficiency (a) and uptake capacity of different reactive dyes (b).

3.7 Adsorption Isotherm

Analyses conducted upon the adsorption theorem enacts an important role in getting an overview of the adsorption mechanism [22]. In this work, isotherm studies were conducted in which the initial concentration of reactive dyes was varied (in the range of 5, 10, 15, 25, 50, 100 mg/L), while pH was maintained constant at 2 and temperature at 35°C. Figure 8 infers that the biochar's uptake capacity gets increased with an increase in the initial concentration of the dye. As

per the figure, the highest experimental uptakes such as 73.44 mg/L, 75.68 mg/g, and 55.37 mg/g were obtained for RO16, RB5, and RB19. The researcher used both the two-parameter model (Freundlich and Langmuir model) and the three-parameter model (Toth model) to fit the reactive dye isotherms. The constants of different models are detailed in Table 3.

In general, the Langmuir model is fit for the experimental uptake if the correlation coefficient is not less than 0.8831. The researcher found the Q0 values i.e., 102.50 mg/g, 90.30 mg/g, and 98.60 mg/g for rice husk-derived biochar in the case of RO16, RB5, and RB19 dyes. In line with this, the affinity constant (b) is in the order of RO16 (0.0326 L/mg) > RB5 (0.0253 L/mg) > RB19 (0.0251 L/mg). Further, the Freundlich model is fit if its correlation coefficient is not less than 0.9570 in the order of RB19 > RB5 > RO16. In the case of the three-parameter Toth model, it can be said as best fit with experimental data if the highest correlation coefficient is not less than 0.8847 in the order of RO16 > RB5 > RB19. Toth model Qmax values were as follows RO16 (117.71 mg/g) > RB19 (93.80 mg/g) > RB5 (89.06 mg/g). As per the discussion, Freundlich Model was found to have the best fit with the experimental values attained.

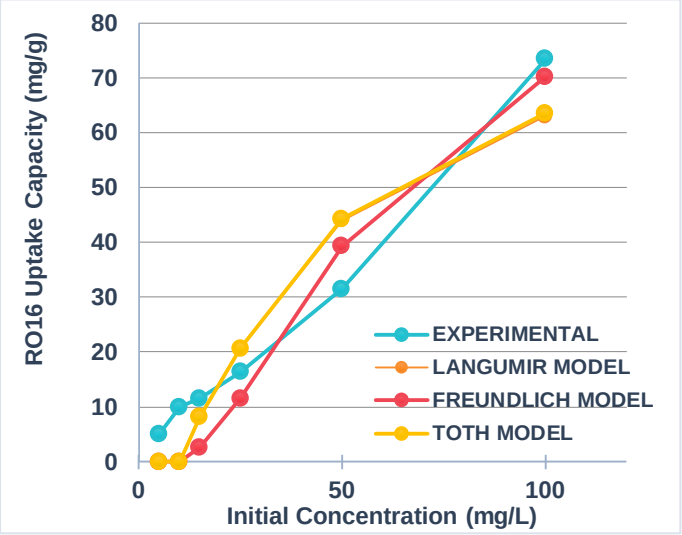

(a)

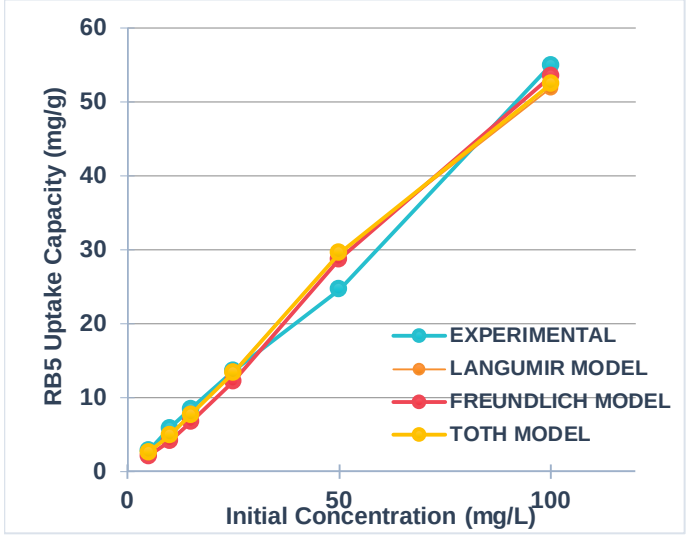

(b)

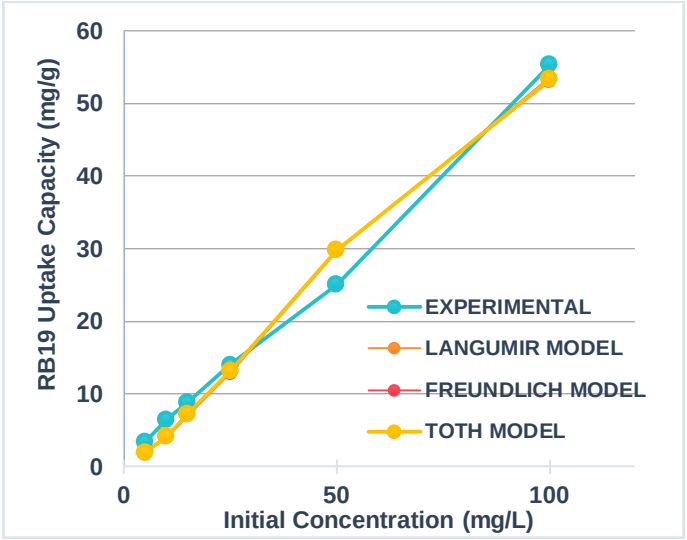

(c)

Figure 8: Predicted uptake of RO16 (a), RB5 (b), and RB19 (c) for rice husk-derived biochar.

Table 3: Adsorption Isotherm constants for RO16, RB5, and RB19.

Adsorption Isotherms Constants for RO16, RB5, and RB19				
Model	Constants	RO16	RB5	RB19
Langmuir Model	Q0	102.500	90.300	98.600
	b	0.033	0.025	0.025
	R2	0.883	0.982	0.976
Freundlich Model	KF	0.359	0.864	1.138
	n	0.622	0.924	0.986
	R2	0.957	0.987	0.983
Toth Model	Qmax	117.711	89.062	93.803
	bT	0.020	0.013	0.013
	nT	0.051	0.047	0.045
	R2	0.885	0.983	0.982

3.8 Kinetic Studies

This work conducted the kinetic study under constant pH 2 and temperature 35°C while the initial dye concentration was varied between 5 mg/L and 100 mg/L and time intervals varied between 0-360 minutes. Figure 9 shows the uptake capacity of biochar under varying initial concentrations at different time intervals. Biochar attained the highest uptake capacity and maximum removal efficiency within 120 minutes. There was a less increase observed in uptake capacity with time expansion. For instance, RB5 recorded 74.98 mg/g uptake capacity at 120 minutes whereas it increased to 75.68 mg/g at 360 minutes i.e., 0.7 mg/g difference between 120 and 360 minutes for an initial concentration of 100 mg/L. Thus, the kinetic study results confirmed that vigorous adsorption occurs at first 120 minutes while the uptake capacity was less intensive, thereafter. So, the equilibrium time is fixed as 120 minutes for all the dyes. Both pseudo-first-order and pseudo-second-order models were involved in identifying the best fit model for experimental data of the kinetic study. In Table 4, the constants for various reactive dyes and two kinetic models are shown. It is found that the pseudo-first-order model had a correlation coefficient of not less than 0.9548, whereas it was not less than 0.9278 in the case of the pseudo-second-order model.

Table 4: Kinetics parameters of pseudo-first-order kinetics and pseudo-second-order kinetics model for RO16, RB5 and RB19

Kinetic Model	Dye	Constant	5 mg/L	15 mg/L	25 mg/L	50 mg/L	100 mg/L
Pseudo First Order Kinetics	RO16	Qe	5.012	11.460	15.507	30.467	70.527
		k1	0.176	0.031	0.068	0.122	0.169
		R2	0.999	0.988	0.961	0.986	0.970
	RB5	Qe	2.784	8.601	13.365	24.441	71.502
		k1	0.020	0.019	0.034	0.024	0.136
		R2	0.984	0.959	0.993	0.991	0.955
	RB19	Qe	3.285	9.031	13.808	24.870	56.887
		k1	0.027	0.021	0.036	0.025	0.019
		R2	0.964	0.957	0.991	0.990	0.956
Pseudo Second Order Kinetics	RO16	Qe	5.114	11.987	16.638	31.843	73.431
		k1	0.114	0.004	0.007	0.008	0.005
		R2	0.990	0.983	0.994	0.998	0.992
	RB5	Qe	3.249	10.117	14.811	27.949	75.405
		k1	0.007	0.002	0.003	0.001	0.003
		R2	0.979	0.942	0.989	0.988	0.989
	RB19	Qe	3.676	10.465	15.239	28.331	68.002
		k1	0.010	0.002	0.003	0.001	0.000
		R2	0.976	0.944	0.990	0.989	0.928

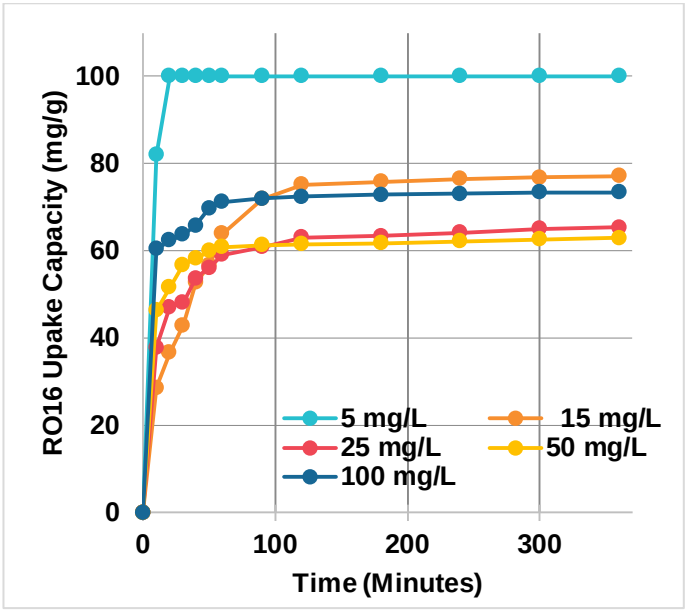

(a)

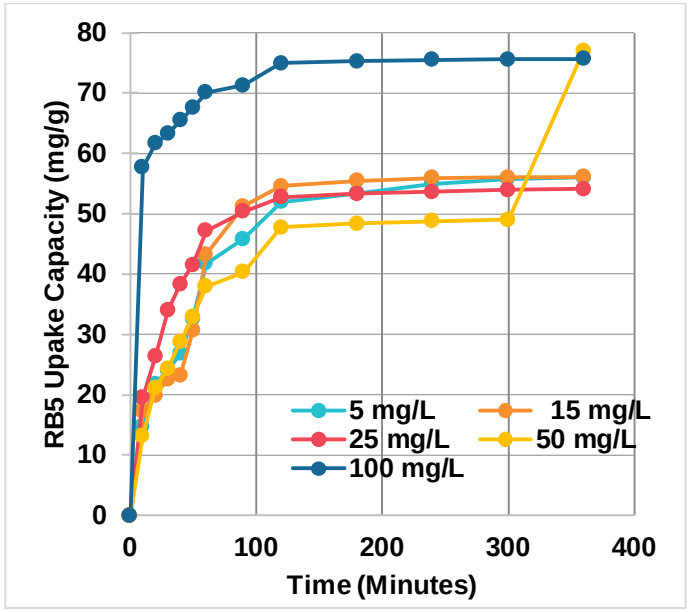

(b)

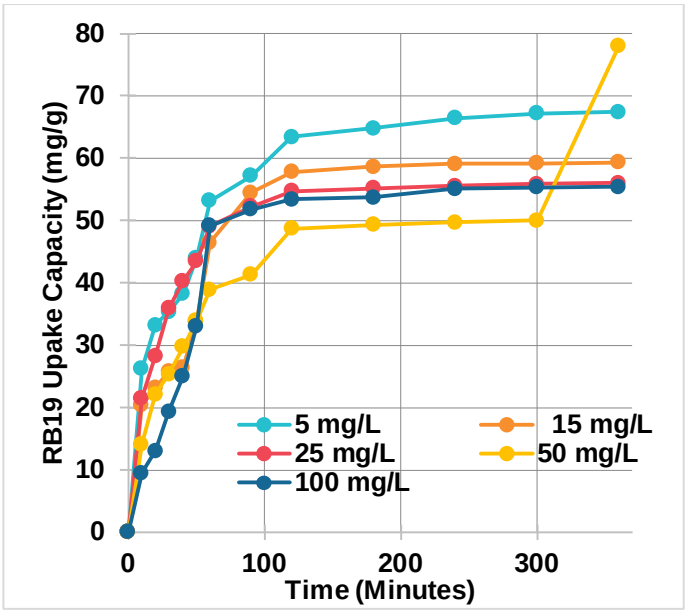

(c)

Figure 9: Experimental uptake of RO16 (a), RB5 (b), and RB19 (c) for rice husk-derived biochar.

3.9 Regeneration Studies

The success of a sorbent is decided based on its reusability efficiency since it is correlated with the cost incurred upon treatment. So, sorbent reusability should be investigated during the adsorption process. The researchers conducted a desorption study to identify the best elutant with S/L ration and regeneration cycles. The desorption efficiencies of various elutants are shown in Figure 10(a). Sodium Hydroxide was identified as the best elutant among available ones since its desorption efficiency was maximum i.e., 99.4%, 99.7%, and 99.6% for RO16, RB5, and RB19 respectively. The order of desorption efficiency for elutants used is as follows Sodium Hydroxide (NaOH) > sodium carbonate (Na_2CO_3) > ammonium hydroxide (NH_4OH) > hydrochloric acid (HCl) > Methanol (CH_3OH). Then, the researcher investigated the sorbent-to-elutant ratio to identify the optimum volume of elutant that should be utilized for desorption purposes. The S/L ratio is shown in Figure 10 (b) which concludes that there are no significant changes up to 5 S/L ratios. However,

the desorption efficiency got declined to 95.2%, 95.1%, and 94.1% for RO16, RB5, and RB19 correspondingly, when the S/L ratio was increased to 6.6. Gokulan et al., 2019 attained the same observation too earlier [25]. Finally, the sorption-elution process was analysed for regeneration cycles. Figure 10 (c) clarifies that no significant changes were observed in desorption efficiency up to cycle 4 which remained higher than 98.1% for all three reactive dyes. However, during cycle 5, a notable decline was observed in desorption efficiency i.e., 95.6%, 94.9%, and 95.2% for the dyes under study. So, the results conclude that rice husk-derived biochar can be successfully used up to four sorption-elution cycles.

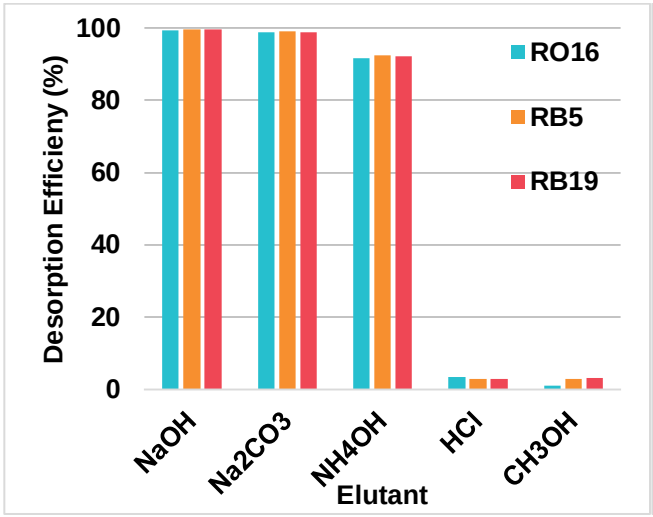

(a)

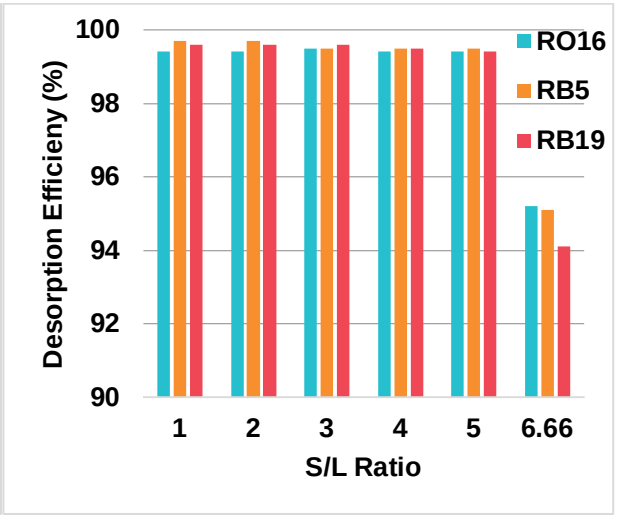

(b)

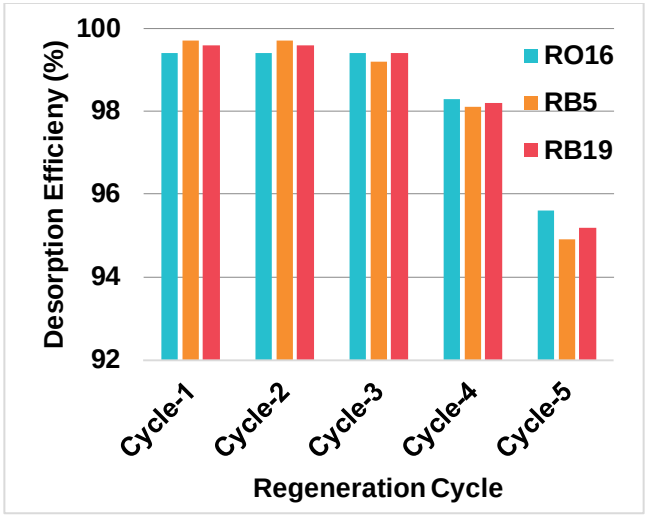

(c)

Figure 10: Desorption efficiency of different elutant (a); S/L ratio (b); Regeneration cycles (c).

4 Conclusion

The present study signifies the usage of biochar derived from rice husk as a practical and efficient solution to treat wastewater containing reactive dyes. The results conclude that dye removal efficiency and uptake capacity were in the order of RO16 > RB5 > RB19. Freundlich Model was predicted to be the best fit model, as per the adsorption isotherm model. Sodium hydroxide has been established with maximum desorption efficiency of 99.4%, 99.7%, and 99.6% for RO16, RB5, and RB19 during reusability studies with an S/L ratio of 5. Further, the results confirmed that

biochar can be reused up to four regeneration cycles (sorption followed by elution). In the future, column study and life cycle assessment should be conducted to assess the capability of biochar on a real-time basis.

5 Availability of Data And Material

Data can be made available by contacting the corresponding author.

6 Acknowledgement

We express our sincere gratitude to Sophisticated Analytical Instrumental Facility (SAIF), Indian Institute of Technology Madras (IITM), Chennai, India for providing Analytical facilities for the characterization of our samples.

7 References

[1] R. Gokulan, G. G. Prabhu, J. Jegan. (2019). Remediation of complex remazol effluent using biochar derived from green seaweed biomass. *International Journal of Phytoremediation*, DOI, 10.1080/15226514.2019.1612845

[2] X. Li, Y.Li. (2019). Adsorptive Removal of Dyes from Aqueous Solution by KMnO4-Modified Rice Husk and Rice Straw. *Journal of Chemistry*, DOI, 10.1155/2019/8359491

[3] M. Doble, A. Kumar A. (2005). *Biotreatment of industrial effluents*, p. 111-122.

[4] K. K. Choy, G. McKay, J. F. Porter. (1999). Sorption of acid dyes from effluents using activated carbon. *Resources, Conservation and Recycling, 27* (1-2), 57-71, DOI, 10.1016/S0921-3449(98)00085-8.

[5] Y. Zhou, L. Zhang, Z. Cheng. (2015). Removal of organic pollutants of organic pollutants from aqueous solution using agricultural wastes. *Journal of Molecular Liquids*, 212, 739-762.

[6] M. T. Yagub, T. K. Sen, S. Afroze, H. M. Ang. (2011). Dye and its removal from aqueous solution by adsorption, a review. *Advanced Colloid Interface Science*, 209, 172-84.

[7] Y. Chen, Y. Zhu, Z. Wang, Y. Li, L. Wang, L. Ding. (2011). Application studies of activated carbon derived from rice husks produced by chemical-thermal process-a review. *Advanced Colloid Interface Science*, 163, 39-52.

[8] M. A. M. Salleh, D. K. Mahmoud, W. A. W. A. Karim, A. Idris. (2011). Cationic and anionic dye adsorption by agricultural solid wastes, a comprehensive review, *Desalination*, 280,1-13.

[9] T. A. H. Nguyen, H. H. Ngo, W. S. Guo, J. Zhang, S. Liang, Q. Y. Yue. (2013). Applicability of agricultural waste and by-products for adsorptive removal of heavy metals from wastewater, *Bio resource Technology*, 148, 574-585.

[10] N. Khan, P. Chowdhary, A. Ahmad, B. S. Giri, P. Chaturvedi. (2020). Hydrothermal liquefaction of rice husk and cow dung in Mixed-Bed-Rotating Pyrolyzer and application of biochar for dye removal, *Bio resource Technology*.

[11] A. K. Silos-Llamas, G. Duran-Jimenez, V. Hernandez-Montoya. (2019). Understanding the adsorption of heavy metals on oxygen-rich biochars by using molecular simulation, *Journal of Molecular Liquids*, DOI, 10.1016/j.molliq.2019.112069

[12] L. Leng, X. Yuan, G. Zeng, J. Shao, X. Chen, Z. Wu, H. Wang, X. Peng. (2015). Surface characterization of rice husk bio-char produced by liquefaction and application for cationic dye (Malachite green) adsorption, *Fuel*, 155, 77-85.

[13] A. Ahmad, N. Khan, B. S. Giri, P. Chowdhary, P. Chaturvedi. (2020). Removal of methyelene blue dye using rice husk, cow dung and sludge biochar, Characterization, application, and kinetic studies, *Bioresource Technology*, DOI, 10.1016/j.biortech.2020.123202

[14] F. S. Nworie, F. I. Nwabue, W. Oti, E. Mbam, B.U. Nwali. (2019). Removal of methylene blue from aqueous solution using activated rice husk biochar, adsorption isotherms, kinetics and error analysis, *Journal of the Chilean chemical society, 64*(1), 4365-4376.

[15] J. Jegan, S. Praveen, T. B. Pushpa, R. Gokulan. (2020). Sorption kinetics and isotherm studies of cationic dyes using groundnut (Arachis hypogaea) shell derived biochar-a low-cost adsorbent. *Applied ecology and environmental research,* 8(1), 1925-1939.

[16] R. Gokulan, A. Avinash, G. G. Prabhu, J, Jegan. (2019). Detoxification of remazol dyes by biochar derived from Caulerpa scalpelliformis-an eco-friendly approach. *Journal of Environmental Chemical Engineering.*

[17] Z. Aksu, S. S. Cagatay. (2006). Investigation of biosorption of Gemazol Turquise Blue-G reactive dye by dried Rhizopus arrhizus in batch and continuous systems. *Separation and Purification Technology,* DOI, 10.1016/j.seppur.2005.07.017

[18] M. Sathishkumar, A. Mahadevan, K. Vijayaraghavan, S. Pavagadhi, R. Balasubramanian. (2010). Green recovery of gold through biosorption, biocrystallization, and pyro-crystalization. *Industrial and Engineering Chemistry Research*, 49(16), 7129-7135, DOI,10.1021/ie100104j

[19] R. Gokulan, G. G. Prabhu, J. Jegan. (2019). Remediation of complex remazol effluent using biochar derived from green sea weed biomass. *International Journal of Phytoremediation*, DOI, 10.1080/15226514.2019.1612845

[20] K. Vijayaraghavan, Y. S. Yun. (2008). Competition of Reactive red 4, Reactive orange 16 and Basic blue 3 during biosorption of Reactive blue 4 by polysulfone *-immobilized Corynebacterium glutamicum*. *Journal of Hazardous material*, 153(1-2), 478-486, DOI, 10.1016/j.jhazmat.2007.08.079

[21] G. B. Kankilic, A. U. Metin, I. Tuzun. (2016). Phragmites australis, an alternative biosorbent for basic dye removal. *Ecological Engineering*, 86, 85-94.

[22] G. Ravindiran, R. M. Jeyaraju, J. Josephraj & A. Alagumalai (2019). Comparative Desorption Studies on Remediation of Remazol Dyes using Biochar (Sorbent) derived from green marine seaweeds. *Chemistry Select*, 4(25), 7437-7445.

[23] R. Muralikrishnan, C. Jodhi. (2021). Experimental studies and mathematical modeling of decolorization of Reactive Orange 16 in packed column. *Desalination and Water Treatment*, 217, v-vii, 422-430. DOI, 10.5004/dwt.2021.26909.

[24] R. Muralikrishnan, C. Jodhi. (2020). Biodecolorization of Reactive Dyes Using Biochar Derived from Coconut Shell, Batch, Isotherm, Kinetic and Desorption Studies. *ChemistrySelect*, 5(26). 7734-7742. DOI, 10.1002/slct.202001454.

R.Muralikrishnan is a Research Scholar at the Depatment of Civil Engineering. Annamalai University, Chidambaram, Tamil Nadu, India. His research area is Environmental Engineering.

Dr. C. Jodhi is an Associate Professor at the Department of Civil Engineering, Annamalai University, Chidambaram, Tamil Nadu, India. His research focuses on Wastewater Treatment, Air Pollution and Solid Waste Management.